

Improved Systematic of pp Elastic Scattering Data

V. Uzhinsky¹ and A. Galoyan²

CERN, Geneva, Switzerland

Unified systematic of elastic scattering data (USESD) proposed by the authors (arXiv:1111.4984 [hep-ph]) is based on symmetrized 2-dimensional Fermi distribution for pp elastic scattering amplitude in the impact parameter representation. It allows to describe differential cross sections of the reactions up to $|t| \sim 1.75$ (GeV/c)². To extend it to higher $|t|$ values we consider a two coherent exponential parametrization of the cross sections and show that it cannot describe the cross sections at small $|t|$ at $P_{lab} > 10$ GeV/c. We extract a description of high $|t|$ region from the parameterization and couple it with USESD. As a result, we obtained a good description of all pp elastic scattering data at $P_{lab} > 10$ GeV/c. It can be easily used in Glauber Monte Carlo codes for calculations of nucleus-nucleus interaction properties.

Introduction

Recently, authors of the paper [1] remembered the old parameterization [2] of pp elastic scattering amplitude:

$$f(s, t) = i \left[A_1 e^{B_1 t/2} + A_2 e^{i\phi} e^{B_2 t/2} \right], \quad (1)$$

and applied it for a fitting of the Totem Collaboration data [3] on elastic pp scattering at $\sqrt{s_{pp}} = 7$ TeV. The amplitude was proposed in 1973 by R.J.N. Phillips and V.D. Barger. Nearly at the same time, it was independently proposed and tested in papers [4, 5, 6] where it was applied for a fitting of $\bar{p}p$ elastic scattering.

The authors of the paper [2] analyzed only pp experimental data at $P_{lab} = 12, 14.2, 19.2, 24, 29.7$ GeV/c and at $\sqrt{s_{pp}} = 53$ GeV. No χ^2/Nof and the parameter's errors were given by them. So, a quality of the parameterization is unknown. It's predictive power is unclear.

The authors of the papers [4, 5, 6] fitted antiproton-proton scattering experimental data at $P_{lab} = 1.11 - 16$ [6] GeV/c (twenty-eight sets of data). A fitting of eight selected data sets gave smallest errors. Three coherent exponentials was proposed and used in the paper [7]. There is not any reclamation to technical details of the fittings. We repeated the work and published the results in the paper [8] where we proposed energy dependencies of the parameters.

An advantage of Eq. 1 is that it can be easily applied in Glauber model calculations of hadron-nucleus and nucleus-nucleus interaction properties at high and super high energies, and it can improve an exactness of the calculations. Usually, only one exponent is used in the calculations. The aim of our present paper is a checking of Eq. 1 in a wide range of energies.

There is another parameterization of high energy pp elastic scattering data proposed by us in the paper [9]:

$$f(s, t) = i A \left[R^2 \frac{\pi dq}{\sinh(\pi dq)} \frac{J_1(Rq)}{Rq} + \frac{1}{2q^2} \frac{\pi dq}{\sinh(\pi dq)} \left(\frac{\pi dq}{\tanh(\pi dq)} - 1 \right) J_0(Rq) + \dots \right], \quad q = \sqrt{-t}. \quad (2)$$

It is a Fourier-Bessel transform of a symmetrized 2-dimensional Fermi-function [10],

$$\gamma(\vec{b}) = A \left[\frac{1}{1 + e^{(b-R)/d}} + \frac{1}{1 + e^{-(b+R)/d}} - 1 \right], \quad (3)$$

where $\gamma(\vec{b})$ is the elastic scattering amplitude in the impact parameter representation.

A possibility to describe a high P_T elastic pp scattering was considered in Ref. [9] following papers [11, 12], but we were not satisfied by results. Thus, below we undertake an effort to combine our approach with two coherent exponential one. As a result, we have obtained an improved parameterization of pp elastic scattering data.

¹On leave of LIT, JINR, Dubna, Russia

²On leave of VBLHEP, JINR, Dubna, Russia

1 Validation of two coherent exponential expression

A direct application of Eq. 1 is complicated by strong parameter correlation. Thus, we write a differential elastic scattering cross section using Eq. 1 as:

$$\frac{d\sigma}{dt} = A_1 \left(e^{B_1 t/2} - A_2 e^{B_2 t/2} \right)^2 + A_3 e^{B_2 t}, \quad (4)$$

and fit experimental data at $P_{lab} > 10$ (GeV/c). We took only 45 from 64 sets of experimental data which gave meaningful results. Fit results of the selected data sets are presented in Fig. 1, 2.

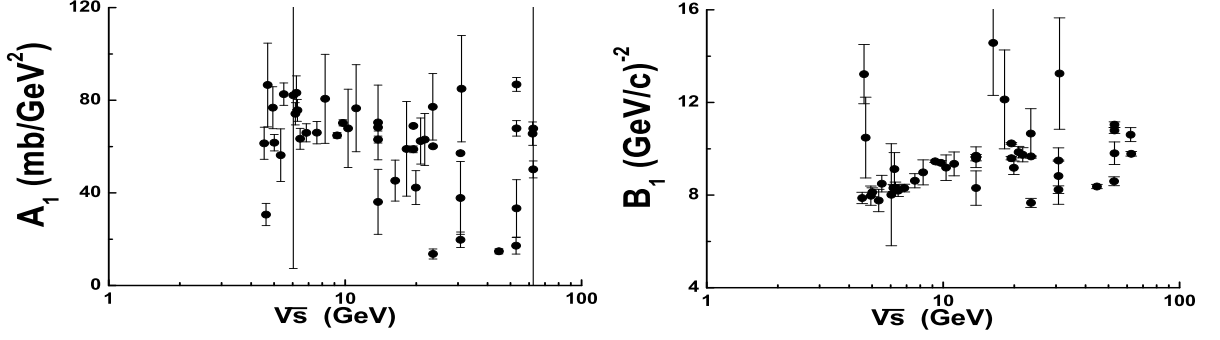


Figure 1: Energy dependencies of the parameters A_1 and B_1 .

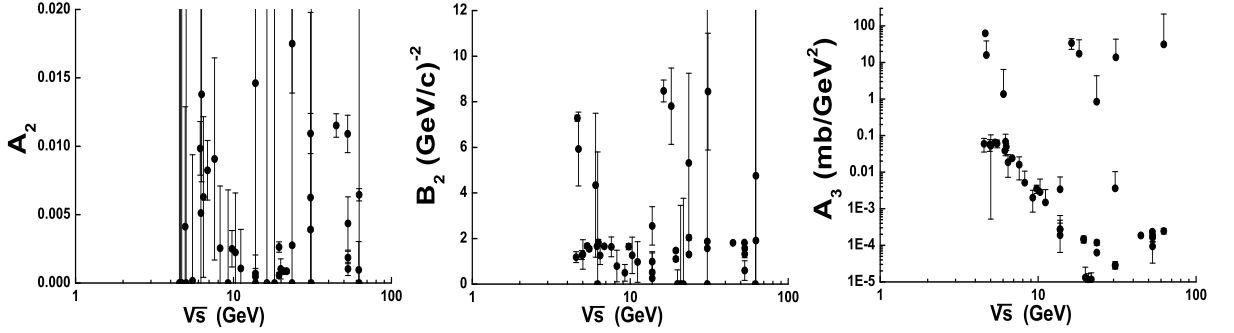


Figure 2: Energy dependencies of the parameters A_2 , B_2 and A_3 .

As seen, the results are rather unstable. Though, $\chi^2/NoF = 2572/1803 \approx 1.43$. Of course, selecting only some experimental data one can obtain stable values of the parameters, as it was done in Ref. [2].

More serious drawback of the parameterization 1 is that it cannot describe small angle scattering data, especially, total cross sections, σ_{tot} , and ratio of real and imaginary parts of elastic scattering amplitude at $t = 0$, $\rho(0) = \text{Re}f(0, s)/\text{Im}f(0, s)$.

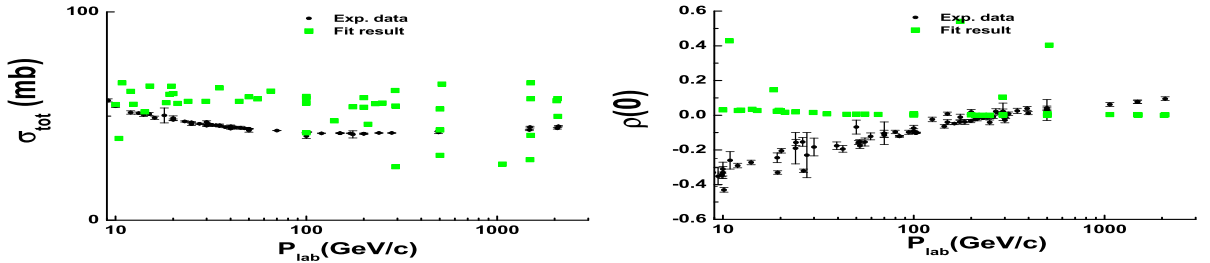


Figure 3: σ_{tot} and $\text{Re}f/\text{Im}f$ as functions of energy. Black points are experimental data from PDG data base [13]. Squares are calculation results without error bars.

Thus, we cannot recommend to use the parameterization for practical calculations.

2 Combination of the approaches

Another situation takes place with the parameterization 2. It describe small angle scattering data rather well, but falls down at large $|t|$. At the same time, the parameterization 1 describes large $|t|$ data quite well. Thus, taking into account that $\phi \sim \pi$ in Eq. 1 we can combine the parameterizations as:

$$Imf(s, t) = A_1 \left[R^2 \frac{\pi dq}{\sinh(\pi dq)} \frac{J_1(Rq)}{Rq} + \frac{1}{2q^2} \frac{\pi dq}{\sinh(\pi dq)} \left(\frac{\pi dq}{\tanh(\pi dq)} - 1 \right) J_0(Rq) \right], \quad (5)$$

$$Ref(s, t) = A_1 \cdot \rho \cdot (R^2/2 + \pi^2 d^2/6) \frac{\pi dq}{\sinh(\pi dq)} J_0(Rq) + A_2 e^{-B_2 q^2/2}, \quad (6)$$

$$\rho = 0.135 - 3/\sqrt{s} + 4/s + 80/s^3, \quad (7)$$

$$\frac{d\sigma}{dt} = 10 \cdot 25.68185 \cdot \pi \cdot (Imf^2 + Ref^2) \quad [mb/(GeV/c)^2], \quad (8)$$

where $q = \sqrt{-t} 25.68185 \text{ [fm}^{-1}\text{]}$, t is 4-momentum transfer $[(GeV/c)^2]$, R and d are in $[fm]$, A_2 is in $[fm^2]$. The parameter A_1 was introduced in order to take into account uncertainties in absolute normalization of experimental data. Experimental data on ρ [13] were approximated by Eq. 7.

There are a lot of experimental data, but most of them are small angle ones. They do not allow an unambiguous determination of the parameters. Thus, we select data at $p_{lab} = 14.2, 19.2, 24, 200, 293, 501 \text{ GeV}/c$ [14], and $\sqrt{s} = 44.7, 52.9, 62.5, \text{ and } 7000 \text{ GeV}$ [15, 3] in which regions of minimum at $|t| \sim 1.5 \text{ (GeV}/c)^2$ and high $|t|$ tails are presented.

Results of the fit ($\chi^2/NoF = 1.51$) of the parameters A_2 and B_2 are presented in Fig. 4.

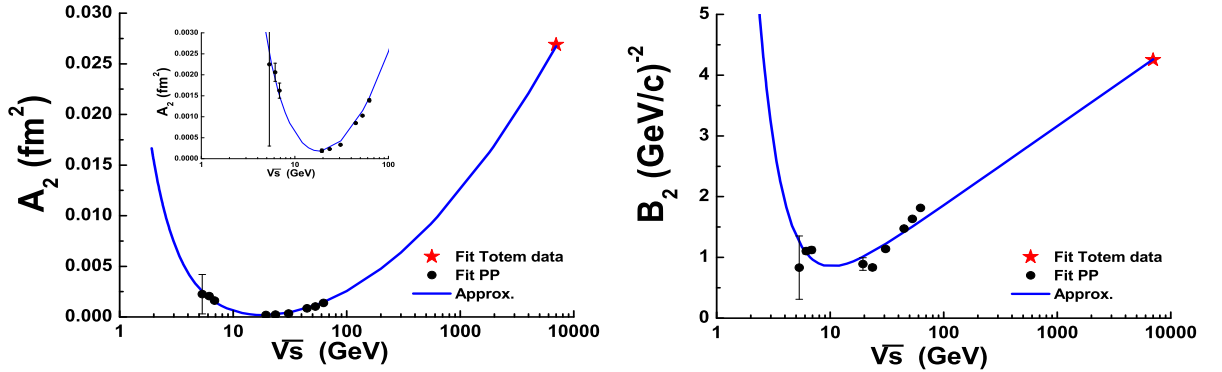


Figure 4: Points are fit results for A_2 and B_2 . Lines are approximations of the energy dependencies.

The energy dependencies of the parameters can be approximated as:

$$A_2 = 1.77 \cdot 10^{-4} [\log(s/225)]^2 + 0.05/s, \quad B_2 = 0.283 \cdot \log(s) + 30/s - 0.75. \quad (9)$$

A change of the sign of A_2 in Eq. 6 from "+" to "-" makes the fit worse.

Having the result for high $|t|$ values we can now determine "soft" parameters (A_1 , R and d) more exactly than it was done before. In our paper [9] we found the parameters at an artificial restriction on "soft" amplitude application region (Eq. 5), $|t| < 1.75 \text{ (GeV}/c)^2$. Now we fix A_2 and B_2 by Eq. 9, and fit other parameters using 64 sets of experimental data (see references in [9]). Results of the fitting are presented in Fig. 5 ($\chi^2/NoF = 1.96$).

As seen, energy dependencies of R and d are determined rather well. They can be parameterized as:

$$R = 0.9/s^{0.25} + 0.053 \log(s), \quad d = 0.379 - 0.26/s^{0.25}. \quad (10)$$

Fitted values of A_1 scatter rather strong especially at low energies. We propose the following parameterization of its energy dependence:

$$A_1 = 1.077 - 0.175 e^{-0.001s^{0.5}} + 0.45/s^{0.25}, \quad (11)$$

According to Eq. 2 total cross section is given as:

$$\sigma_{tot} = 2\pi A_1 (R^2 + \pi^2 d^2/3). \quad (12)$$

If we use only fitting results for A_1 , R , and d , we obtain green points in Fig. 6 shown without error bars. As seen, they are scattered rather strong.

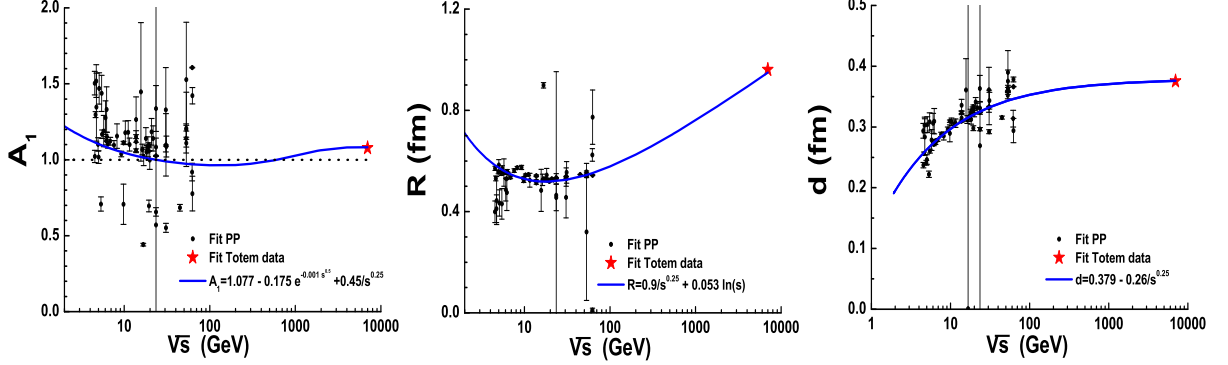


Figure 5: Points are fit results. Lines are approximations of the energy dependencies.

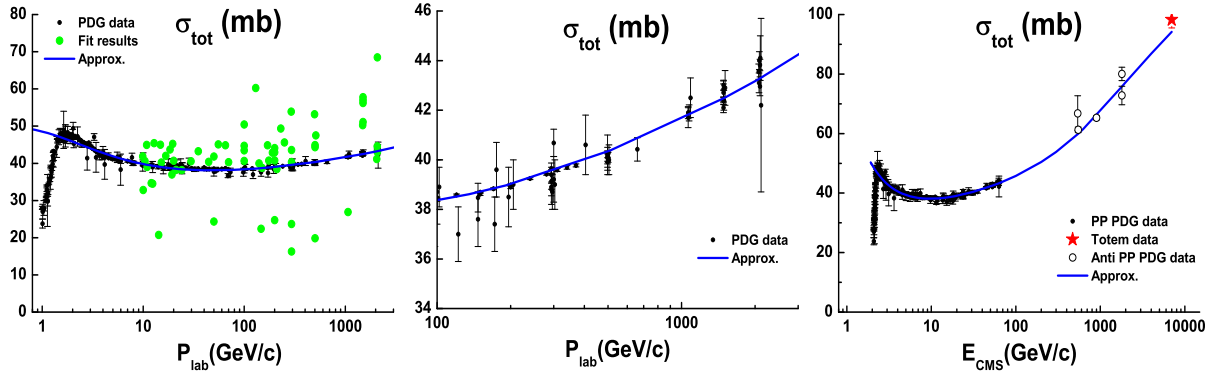


Figure 6: Open and closed points are experimental data from PDG [13] data base. Lines are calculation results using approximations of A_1 (see text).

Using the approximations given by Eqs. 7, 9, and 10 (A_1 was not fixed) we have $\chi^2/NoF = 8179/2256 \simeq 4.79$. A fixing of A_1 by Eq. 11 leads to an increasing of χ^2/NoF in 2 times. A quality of the experimental data descriptions is presented in Appendix A.

3 Application of USESD in Glauber Monte Carlo codes

Glauber Monte Carlo codes [16, 17] (see review in [18]) calculate various properties of inelastic nucleus-nucleus interaction such as: number of participating nucleons, multiplicity of intra-nuclear collision, impact parameter distributions and so on. Mainly they use so-called "nucleon inelastic overlap function", $g(b)$, in the simplest form:

$$g(b) = \theta(R_{int} - b), \quad R_{int} = \sqrt{\sigma_{in}/\pi}. \quad (13)$$

In the Glauber theory the function is given as:

$$g(b) = \gamma(b) + \gamma^*(b) - |\gamma(b)|^2. \quad (14)$$

According to Eqs. 5, 6,

$$\gamma(b) = A_1 \left\{ \frac{e^{-(b-\bar{R})/d}}{1 + e^{-(b-\bar{R})/d}} + \frac{1}{1 + e^{-(b+\bar{R})/d}} - 1 \right\} - \quad (15)$$

$$\begin{aligned}
& -i \rho A_1 \frac{\tilde{R}^2/2 + \pi^2 d^2/6}{\tilde{R}d} \left\{ \frac{e^{-(b-\tilde{R})/d}}{\left[1 + e^{-(b-\tilde{R})/d}\right]^2} + \frac{e^{-(b+\tilde{R})/d}}{\left[1 + e^{-(b+\tilde{R})/d}\right]^2} \right\} - \\
& \quad -i \frac{A_2}{2\pi B_2} e^{-b^2/(2 B_2)} e^{-25.64} \\
& \quad \tilde{R} = R + (0.07 + d + 0.2d^2) e^{-1.2R/d}.
\end{aligned} \tag{16}$$

A reason of the introduction of \tilde{R} is that Eq. 2 was obtained from Eq. 3 assuming $d/R \ll 1$. As seen from the fitting results it is not true for pp interactions. Thus, the correction of Eq. 16 was found at numerical investigation.

Conclusion

USESD is enlarged by the simple description of high $|t|$ elastic scattering. The new parameters have been determined. Exact formulae are presented.

References

- [1] A. Grau, S. Pacetti, G. Pancheri, and Y.N. Srivastava, Phys. Lett., **B714**, 70 (2012).
- [2] R.J.N. Phillips and V.D. Barger, Phys. Lett., **B46**, 412 (1973).
- [3] The Totem Collaboration (G. Antchev et al.) Europhys. Lett., **96**, 21002 (2011);
The Totem Collaboration (G. Antchev et al.) Europhys. Lett., **95**, 41001 (2011).
- [4] H.B. Crawley, E.S. Hafen and W.J. Kerman, Phys. Rev., **D8**, 2012 (1973).
- [5] H.B. Crawley, W.J. Kerman and F. Ogino, Phys. Rev., **D8**, 2781 (1973).
- [6] H.B. Crawley, N.W. Dean, E.S. Hafen, W.J. Kerman and F. Ogino, Phys. Rev., **D9**, 189 (1974).
- [7] H.B. Crawley, N.W. Dean, and W.J. Kerman, Phys. Rev., **D9**, 3029 (1974).
- [8] A. Galoyan, J. Ritman, A. Sokolov and V. Uzhinsky, arXiv:0809.3804 [hep-ex] (2008).
- [9] V. Uzhinsky and A. Galoyan, arXiv:1111.4984 [hepph] (2011).
- [10] D.W.L. Sprung and J. Martorell, J. Phys. **A30** (1997) 6525; **A31** (1998) 8973.
- [11] A. Donnachie and P.V. Landshoff, Nucl. Phys., **B231**, 189 (1984).
- [12] E. Martynov, J.R. Cudiel and A. Lengyel, arXiv:1201.4458 [hep-ph] (2012).
- [13] Particle Data Group, <http://pdg.lbl.gov/2009/hadronic-xsections/hadron.html>
- [14] J.V. Allaby et al., Nucl. Phys. **B52**, 316 (1973).
J.V. Allaby et al., Phys. Lett. **B28**, 67 (1968).
A. Schiz et al., Phys. Rev. **D24**, 26 (1981).
G. Fidencaro et al., Nucl. Phys. **B173**, 513 (1980).
U. Amaldi and K.R. Schubert, Nucl. Phys. **B166**, 301 (1980).
- [15] U. Amaldi and K.R. Schubert, Nucl. Phys. **B166**, 301 (1980).
E. Nagy et al., Nucl. Phys. **B150**, 221 (1979).
- [16] B. Alver, M. Baker, C. Loizides, and P. Steinberg, arXiv:0805.4411 [nucl-exp] (2005).
- [17] W. Broniowski, M. Rybczynski, and P. Bozek, Comp. Phys. Commun., **180**, 69 (2009).
- [18] M.L. Miller, K. Reygers, S.J. Sanders and P. Steinberg, Ann. Rev. Nucl. Part. Sci., **57**, 205 (2007).

Appendix A: Comparison of experimental data on pp -interactions with USESD parameterization

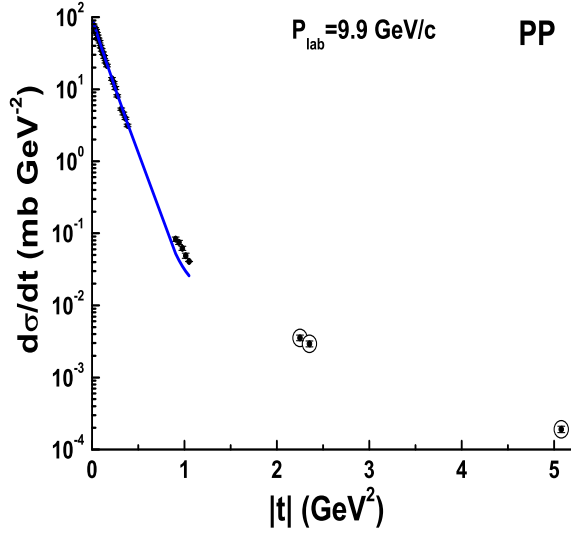


Figure 7: The points are the experimental data by R.M. Edelstein et al., Phys. Rev. **D5** (1972) 1073.

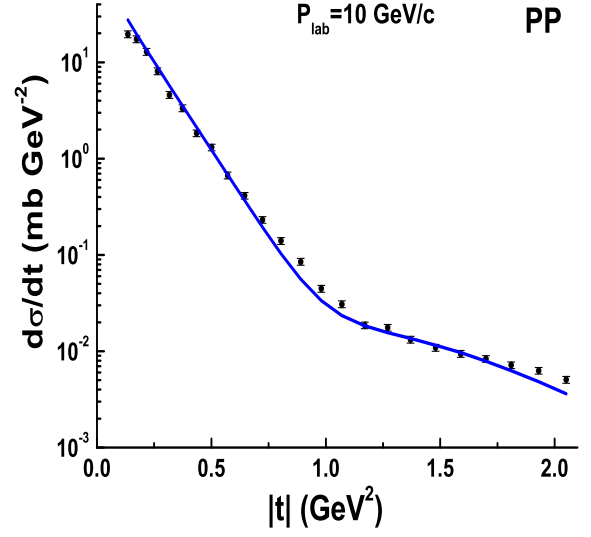


Figure 8: The points are the experimental data by J.V. Allaby et al., Nucl. Phys. **B52** (1973) 316.

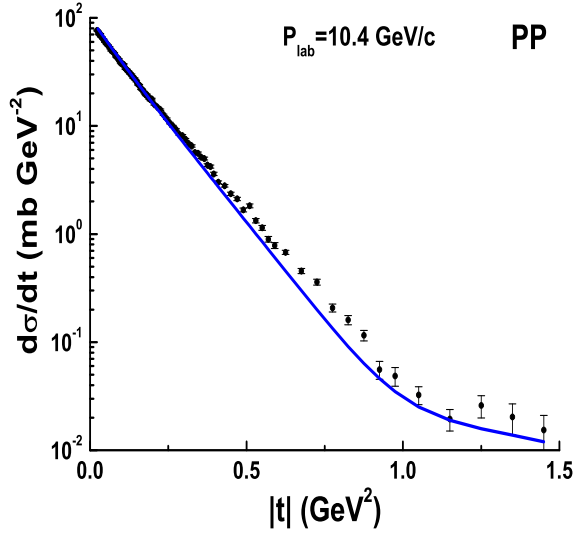


Figure 9: The points are the experimental data by G.W. Brandenburg et al., Phys. Lett. **58B** (1975) 367.

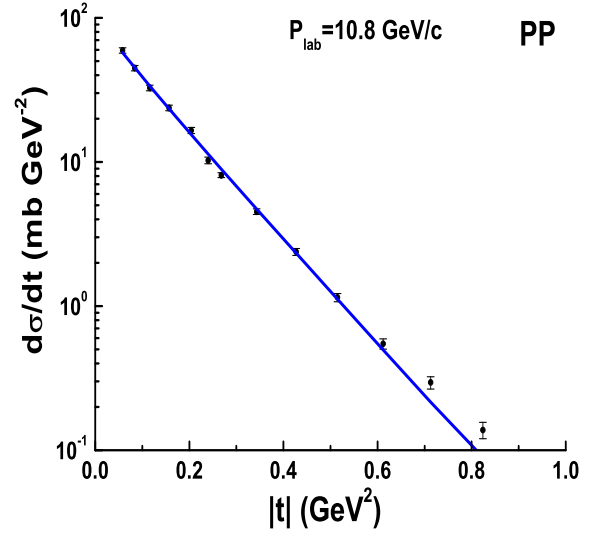


Figure 10: The points are the experimental data by K.J. Foley et al., Phys. Rev. Lett. **11** (1963) 425.

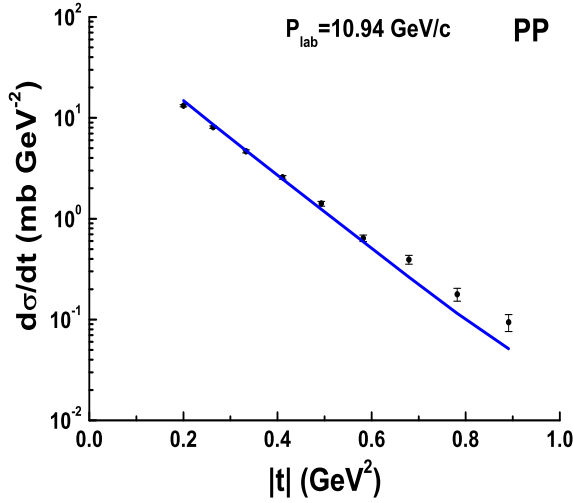


Figure 11: The points are the experimental data by K.J. Foley et al., Phys. Rev. Lett. **15** (1965) 45.

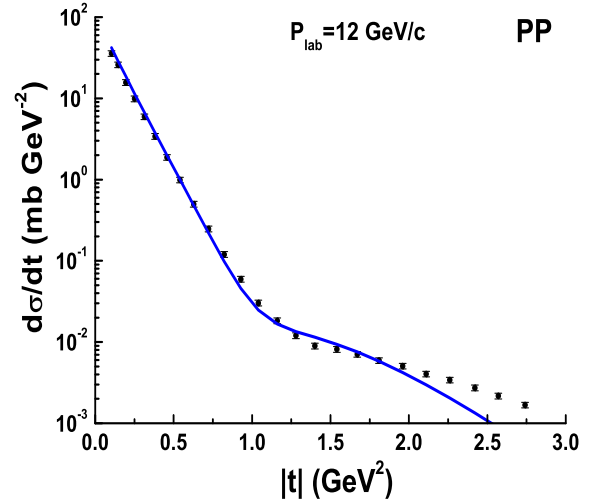


Figure 12: The points are the experimental data by J.V. Allaby et al., Nucl. Phys. **B52** (1973) 316.

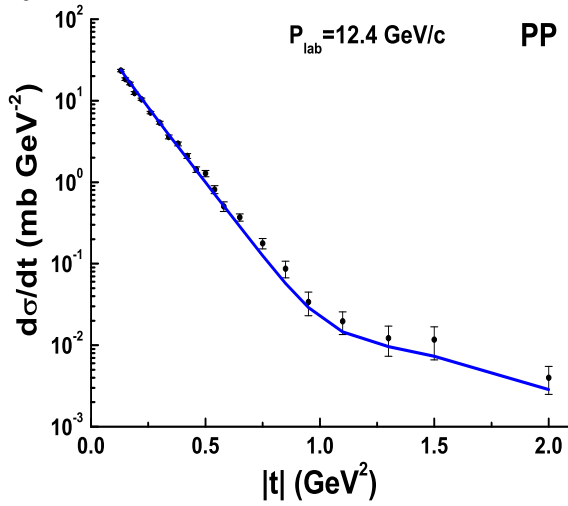


Figure 13: The points are the experimental data by D. Harting, Nuovo Cimento **38** (1965) 60.

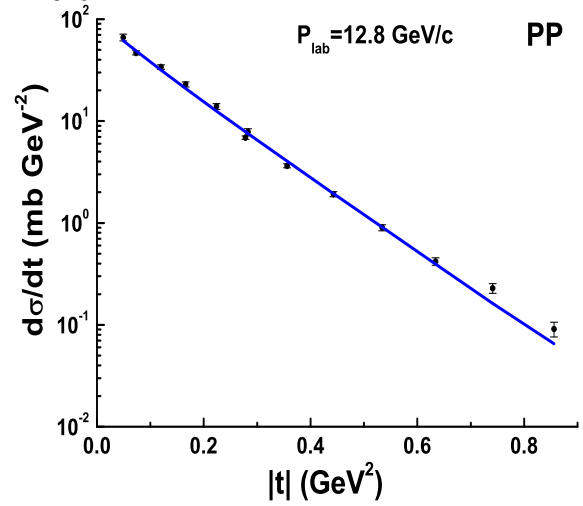


Figure 14: The points are the experimental data by K.J. Foley et al., Phys. Rev. Lett. **11** (1963) 425.

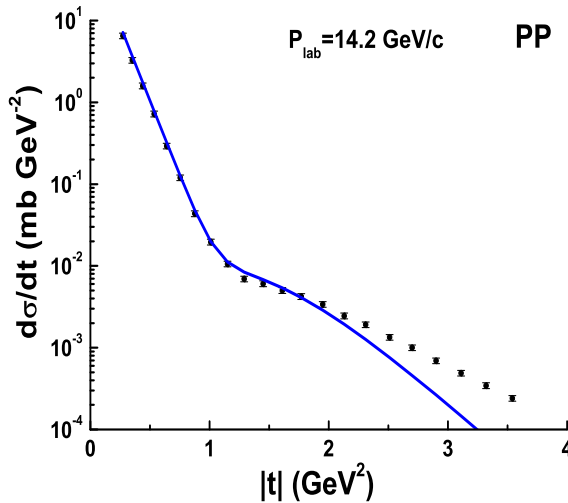


Figure 15: The points are the experimental data by J.V. Allaby et al., Nucl. Phys. **B52** (1973) 316.

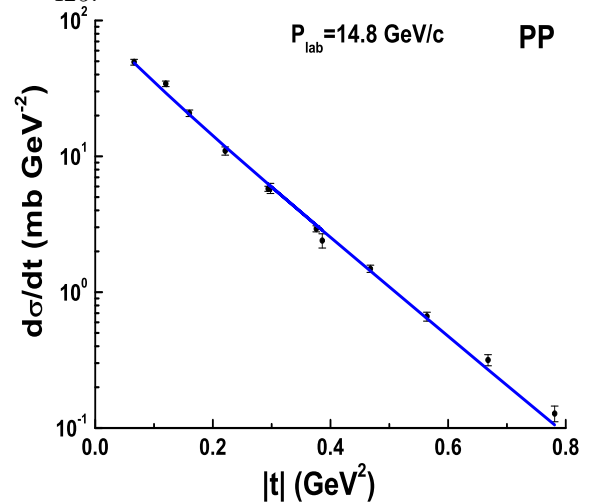


Figure 16: The points are the experimental data by K.J. Foley et al., Phys. Rev. Lett. **11** (1963) 425.

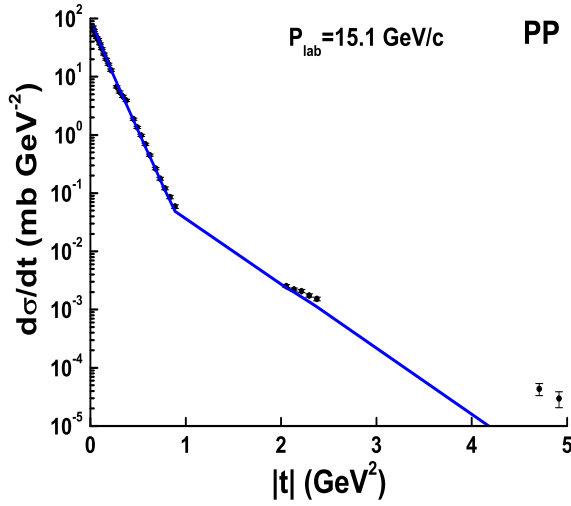


Figure 17: The points are the experimental data by R.M. Edelstein et al., Phys. Rev. **D5** (1972) 1073.

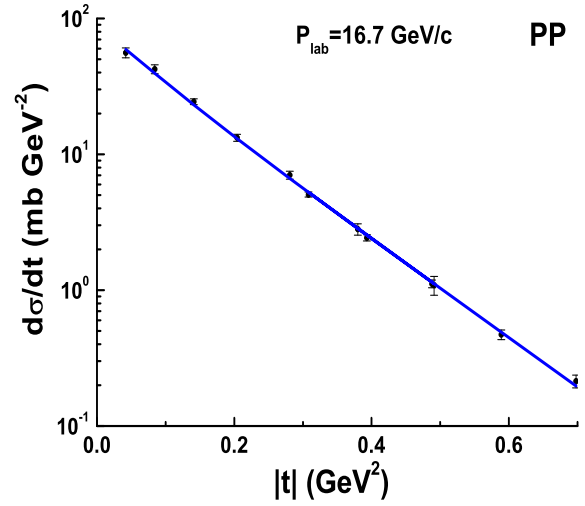


Figure 18: The points are the experimental data by .K.J. Foley et al., Phys. Rev. Lett. **11** (1963) 425

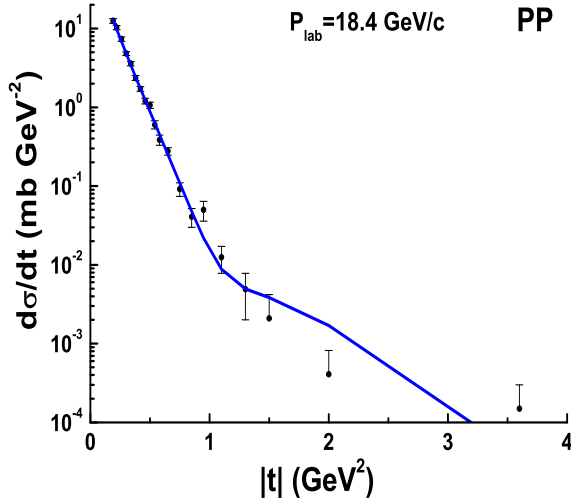


Figure 19: The points are the experimental data by D. Harting, Nuovo Cimento **38** (1965) 60.

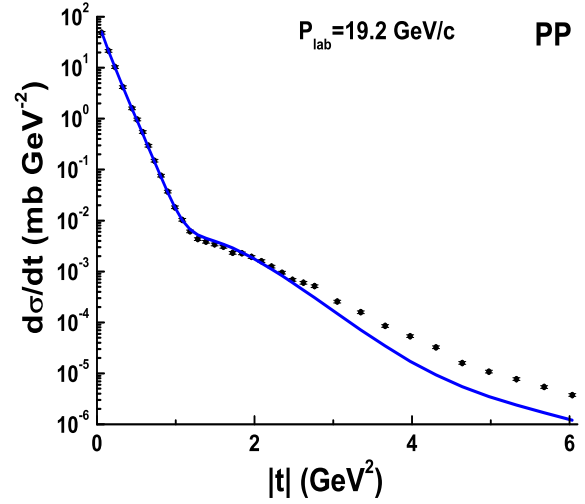


Figure 20: The points are the experimental data by J.V. Allaby et al., Phys. Lett. **B28** (1968) 67.

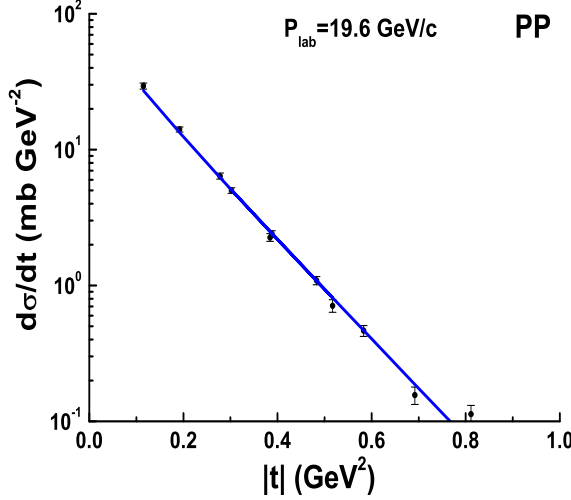


Figure 21: The points are the experimental data by .K.J. Foley et al., Phys. Rev. Lett. **11** (1963) 425

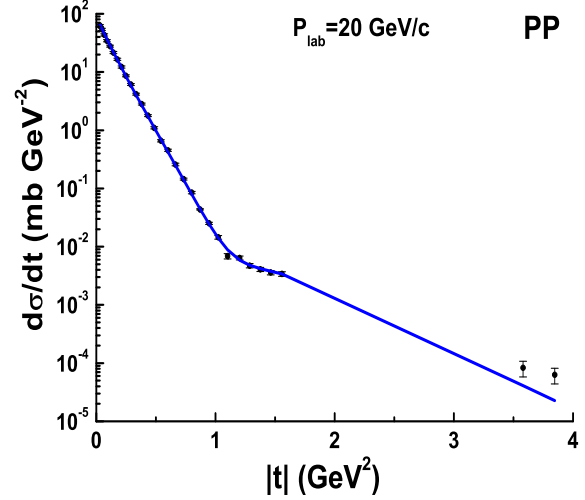


Figure 22: The points are the experimental data by R.M. Edelstein et al., Phys. Rev. **D5** (1972) 1073.

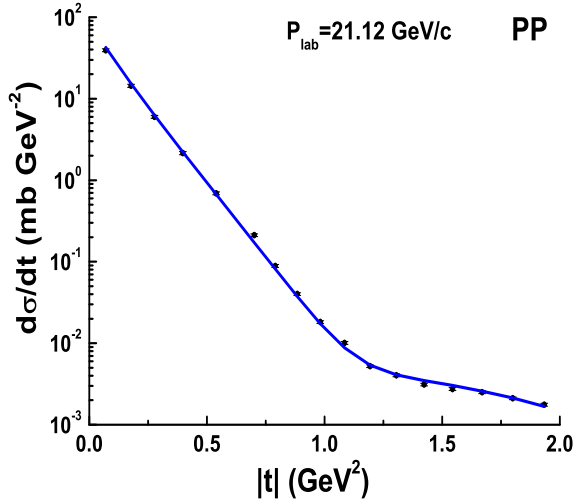


Figure 23: The points are the experimental data by J.V. Allaby et al., Phys. Lett. **B28** (1968) 67.

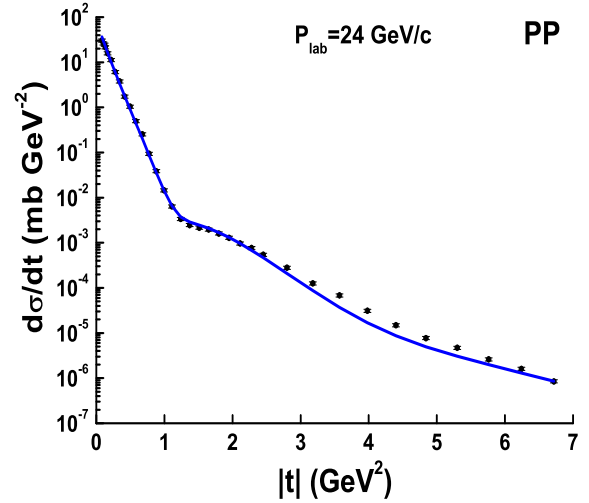


Figure 24: The points are the experimental data by J.V. Allaby et al., Nucl. Phys. **B52** (1973) 316.

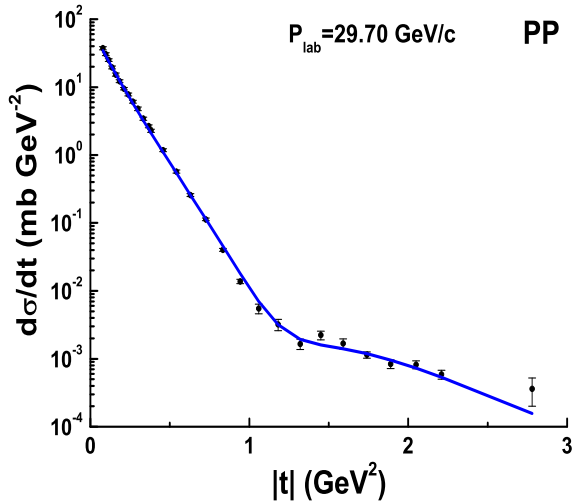


Figure 25: The points are the experimental data by R.M. Edelstein et al., Phys. Rev. **D5** (1972) 1073.

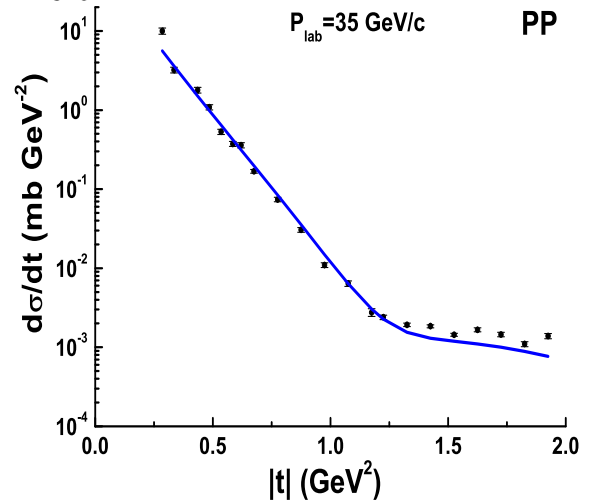


Figure 26: The points are the experimental data by R. Rusack et al., Phys. Rev. Lett. **41** (1978) 1632.

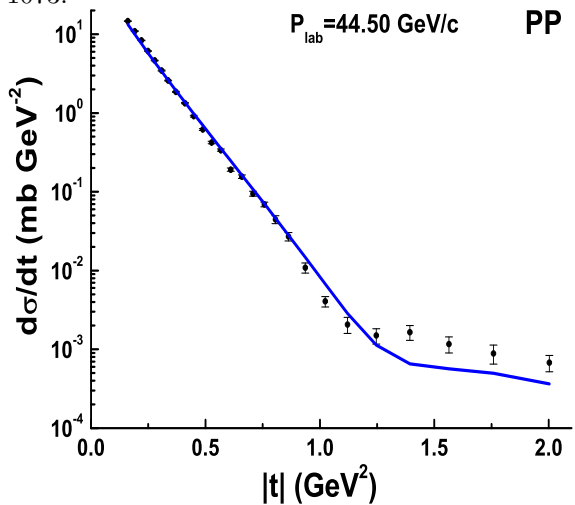


Figure 27: The points are the experimental data by C. Bruneton et al., Nucl. Phys. **B124** (1977) 391.

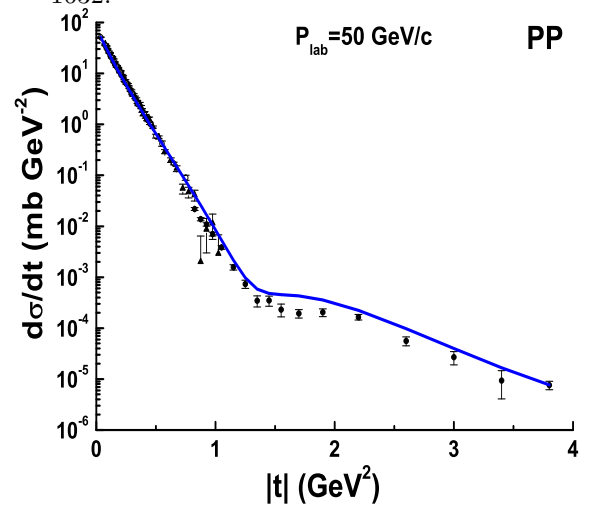


Figure 28: The points are the experimental data by Z. Asad et al., Nucl. Phys. **B255** (1984) 273; C.W. Akerlof et al., Phys. Rev. **D14** (1976) 2864; D.S. Ayres et al., Phys. Rev. **D15** (1977) 3105.

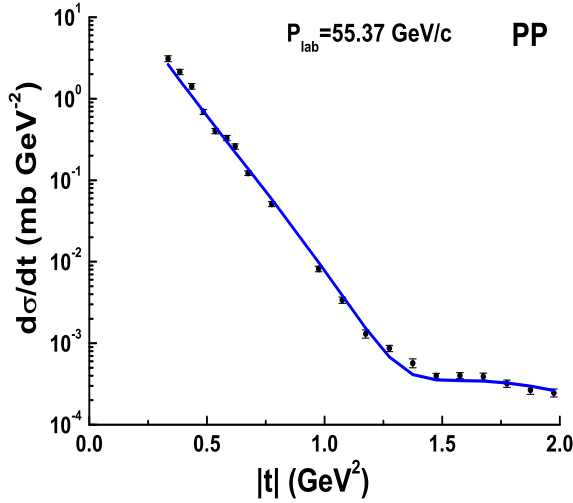


Figure 29: The points are the experimental data by R. Rusack et al., Phys. Rev. Lett. **41** (1978) 1632.

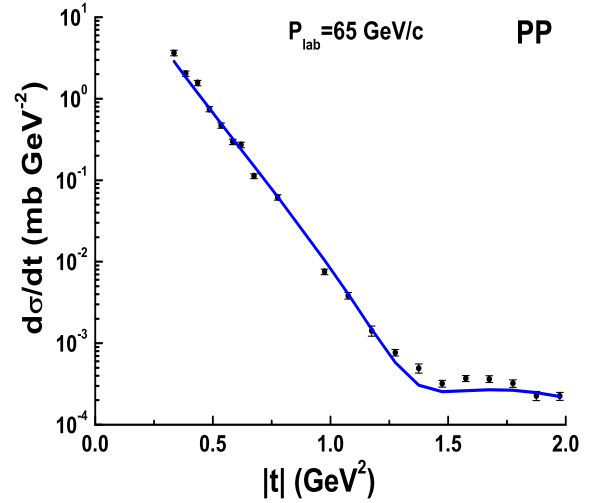


Figure 30: The points are the experimental data by R. Rusack et al., Phys. Rev. Lett. **41** (1978) 1632.

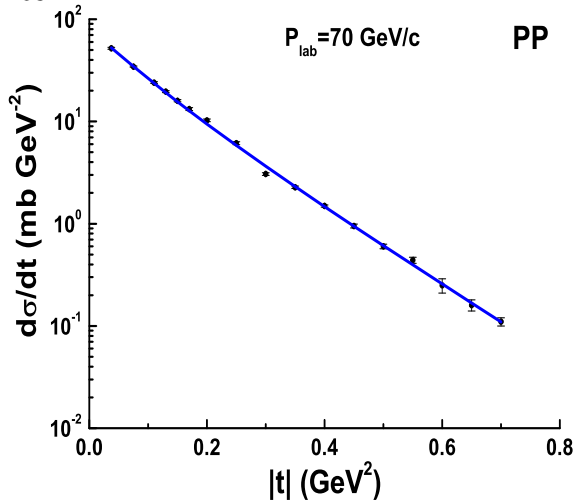


Figure 31: The points are the experimental data by D.S. Ayres et al., Phys. Rev. **D15** (1977) 3105.

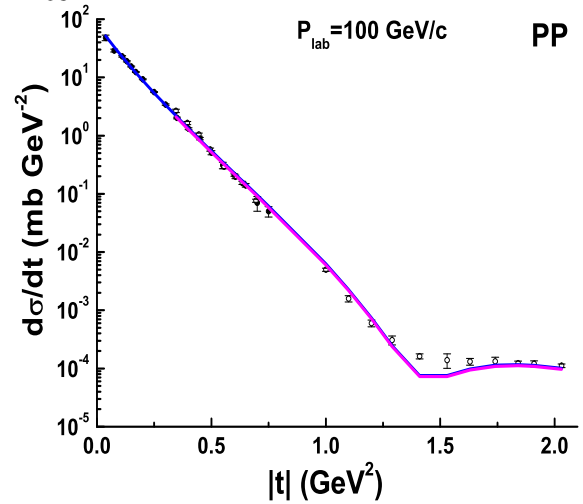


Figure 32: The points are the experimental data by C.W. Akerlof et al., Phys. Rev. **D14** (1976) 2864; R. Rubinstein et al., Phys. Rev. **D30** (1984) 1413.

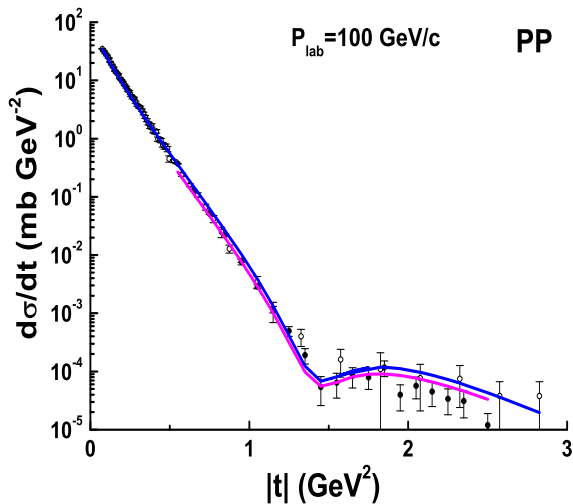


Figure 33: The points are the experimental data by D.S. Ayres et al., Phys. Rev. **D15** (1977) 3105; R. Rusack et al., Phys. Rev. Lett. **41** (1978) 1632.

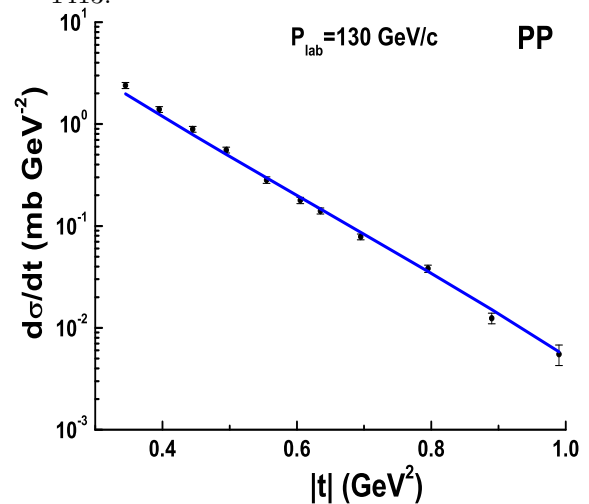


Figure 34: The points are the experimental data by R. Rusack et al., Phys. Rev. Lett. **41** (1978) 1632.

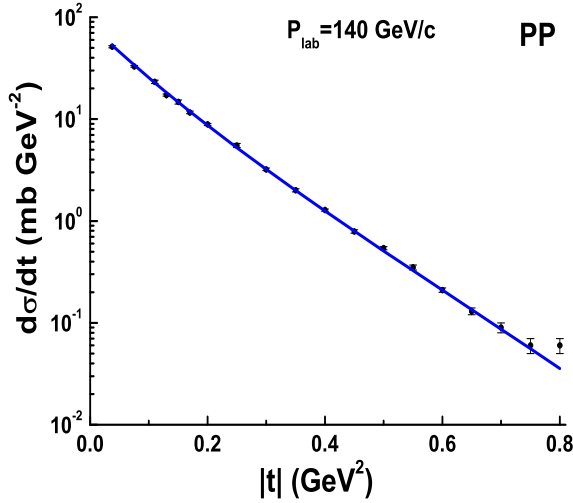


Figure 35: The points are the experimental data by D.S. Ayres et al., Phys. Rev. **D15** (1977) 3105.

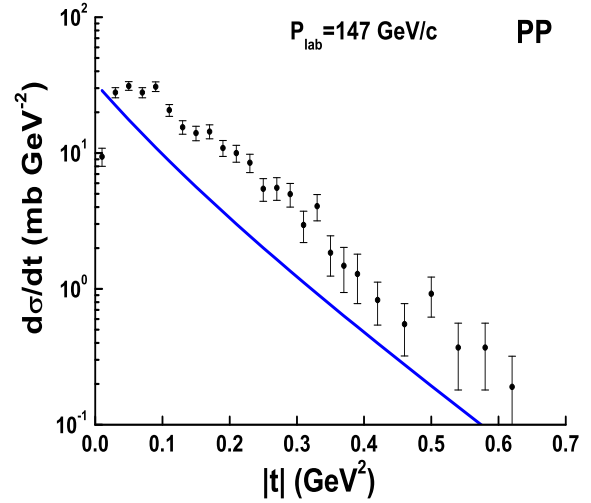


Figure 36: The points are the experimental data by D. Brick et al., Phys. Rev. **D25** (1982) 2794.

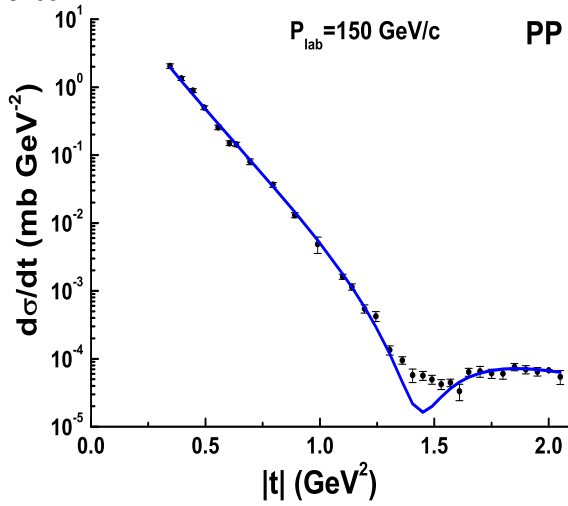


Figure 37: The points are the experimental data by R. Rusack et al., Phys. Rev. Lett. **41** (1978) 1632.

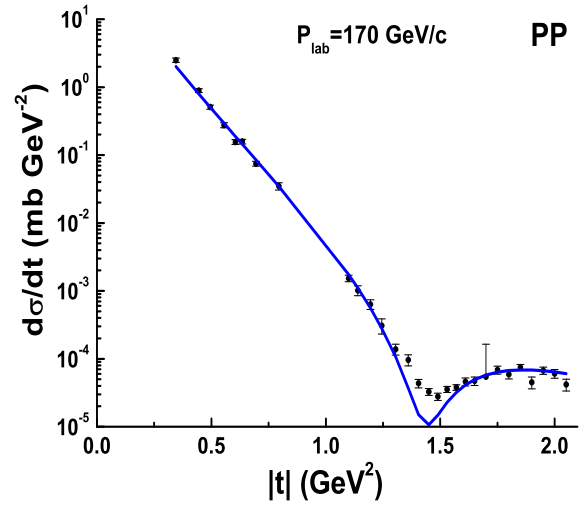


Figure 38: The points are the experimental data by R. Rusack et al., Phys. Rev. Lett. **41** (1978) 1632.

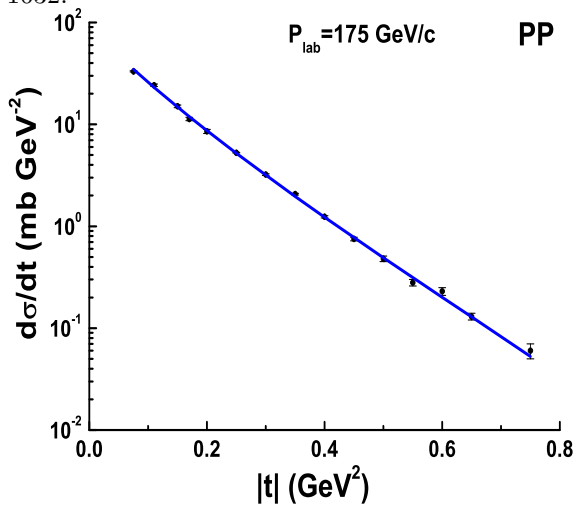


Figure 39: The points are the experimental data by D.S. Ayres et al., Phys. Rev. **D15** (1977) 3105.

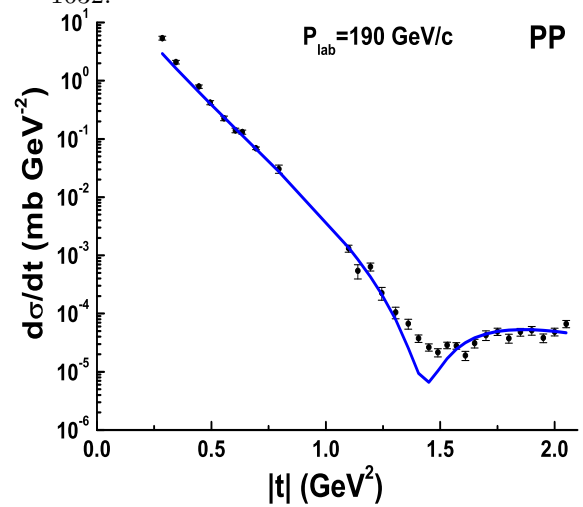


Figure 40: The points are the experimental data by R. Rusack et al., Phys. Rev. Lett. **41** (1978) 1632.

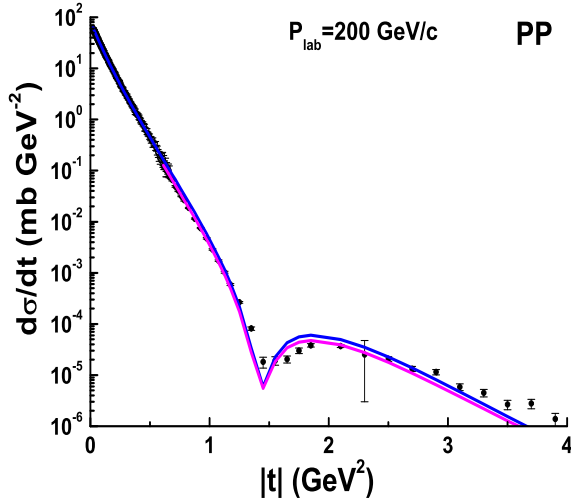


Figure 41: The points are the experimental data by C.W. Akerlof et al., Phys. Rev. **D14** (1976) 2864; R. Rubinstein et al., Phys. Rev. **D30** (1984) 1413.

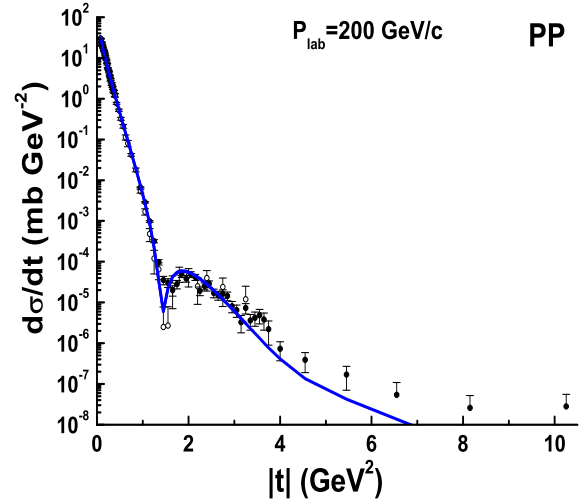


Figure 42: The points are the experimental data by A. Schiz et al., Phys. Rev. **D24** (1981) 26; G. Fidecaro et al., Nucl. Phys. **B173** (1980) 513.

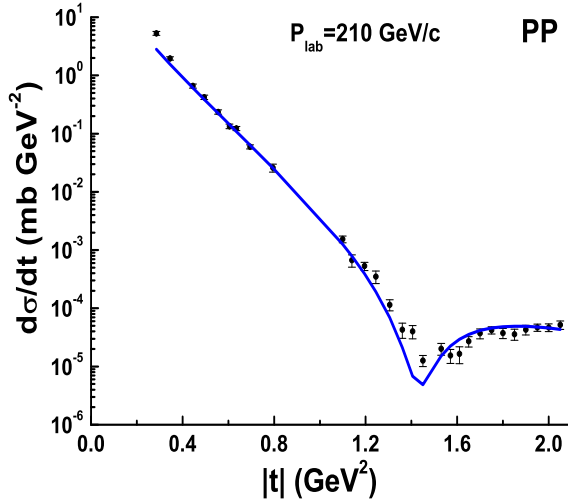


Figure 43: The points are the experimental data by R. Rusack et al., Phys. Rev. Lett. **41** (1978) 1632.

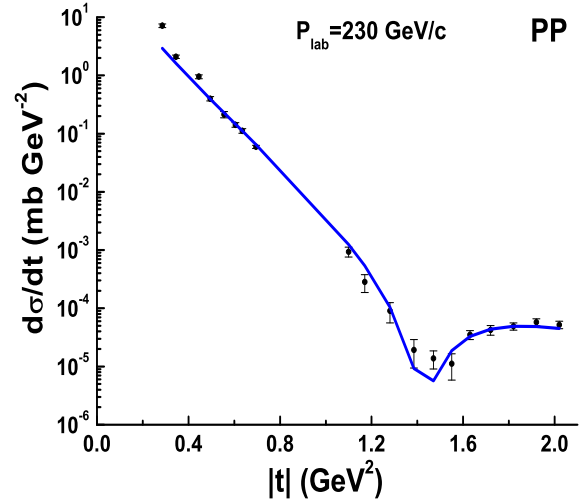


Figure 44: The points are the experimental data by R. Rusack et al., Phys. Rev. Lett. **41** (1978) 1632.

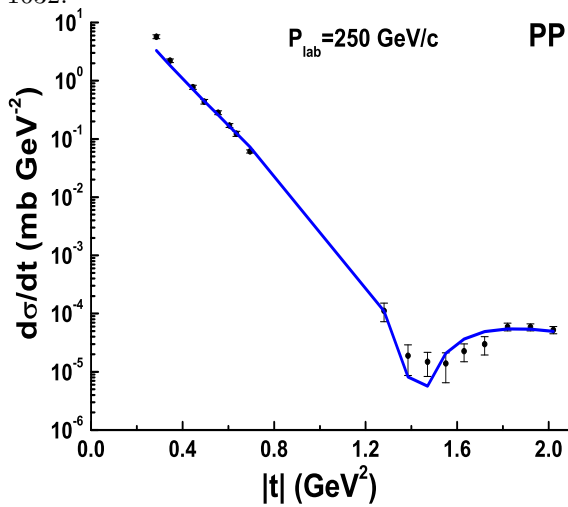


Figure 45: The points are the experimental data by R. Rusack et al., Phys. Rev. Lett. **41** (1978) 1632.

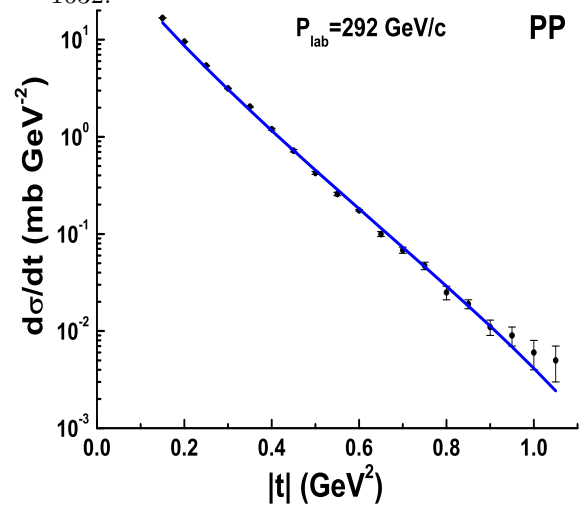


Figure 46: The points are the experimental data by M.G. Albrow et al., Nucl. Phys. **B108** (1976) 1.

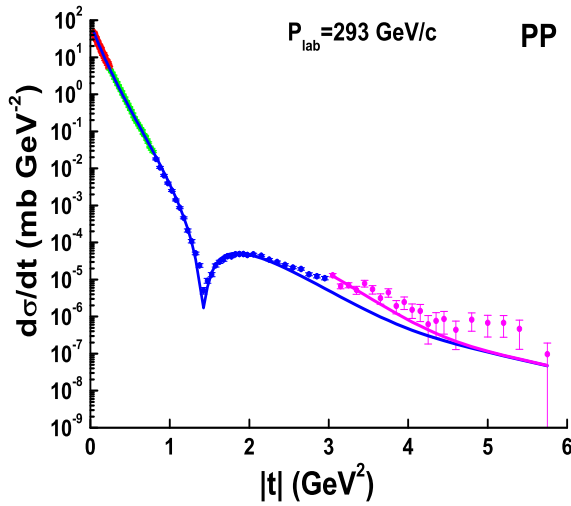


Figure 47: The points are the experimental data by U. Amaldi and K.R. Schubert, Nucl. Phys. **B166** (1980) 301.

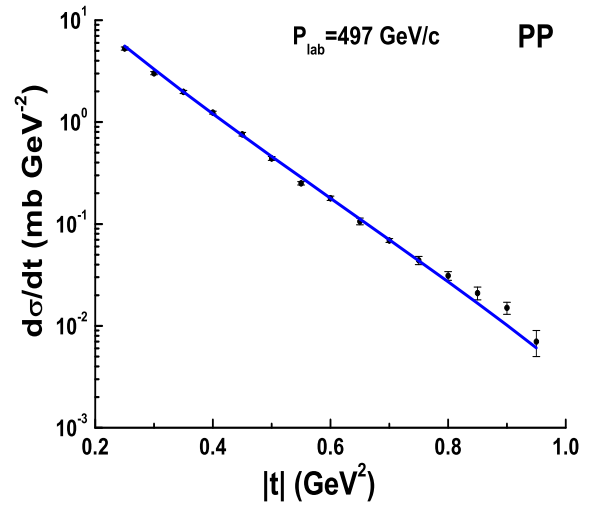


Figure 48: The points are the experimental data by M.G. Albrow et al., Nucl. Phys. **B108** (1976) 1.

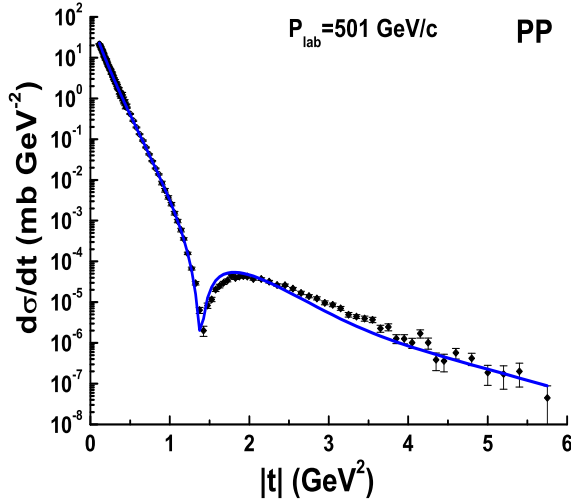


Figure 49: The points are the experimental data by U. Amaldi and K.R. Schubert, Nucl. Phys. **B166** (1980) 301.

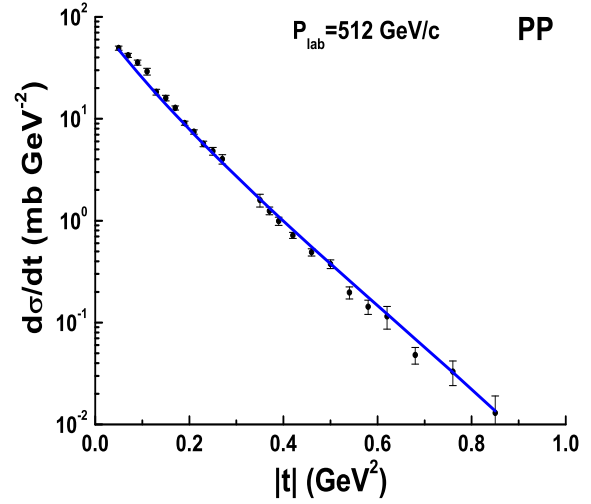


Figure 50: The points are the experimental data by A. Breakstone et al. Nucl. Phys. **B248** (1984) 253.

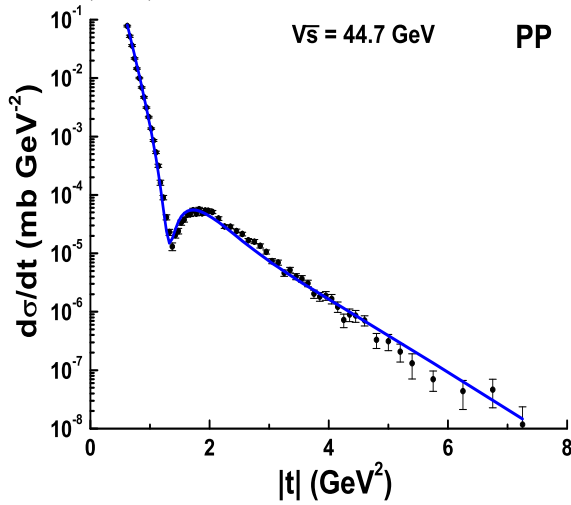


Figure 51: The points are the experimental data by U. Amaldi and K.R. Schubert, Nucl. Phys. **B166** (1980) 301.

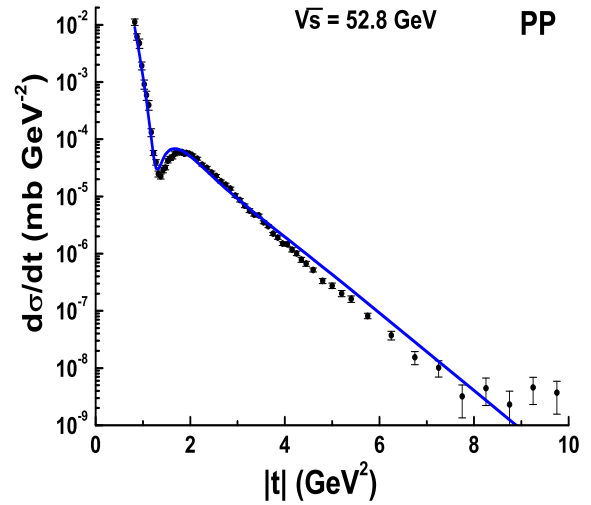


Figure 52: The points are the experimental data by E. Nagy et al., Nucl. Phys. **B150** (1979) 221.

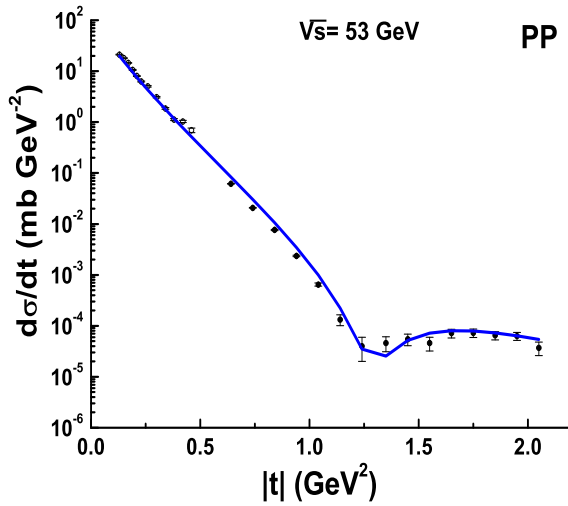


Figure 53: The points are the experimental data by A. Breakstone et al. Nucl. Phys. **B248** (1984) 253; Phys. Rev. Lett. **54** (1985) 2180.

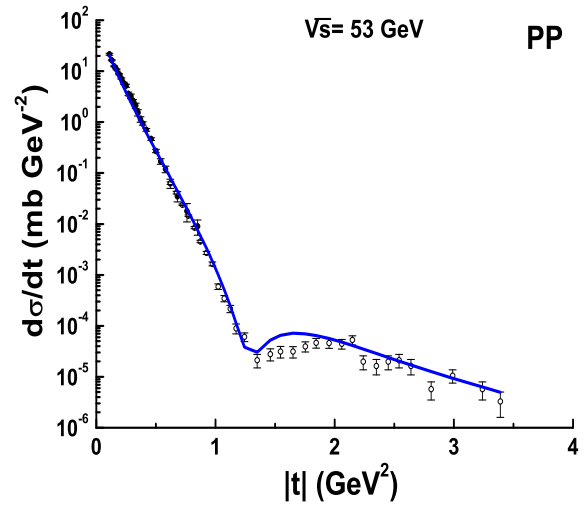


Figure 54: The points are the experimental data by S. Erhan et al., Phys. Lett. **B152** (1985) 131; J.C.M. Armitage et al., Nucl. Phys. **B132** (1978) 365.

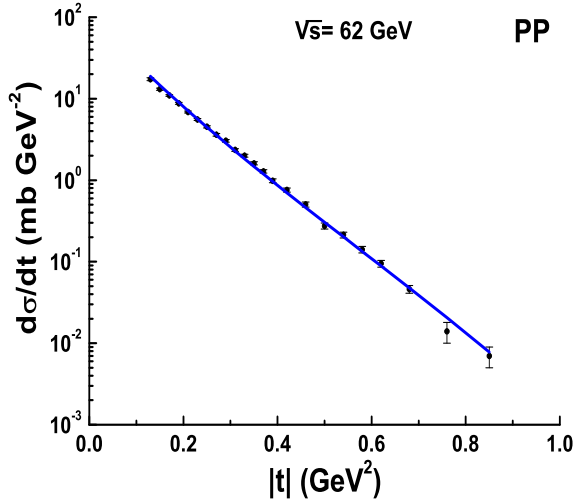


Figure 55: The points are the experimental data by A. Breakstone et al. Nucl. Phys. **B248** (1984) 253.

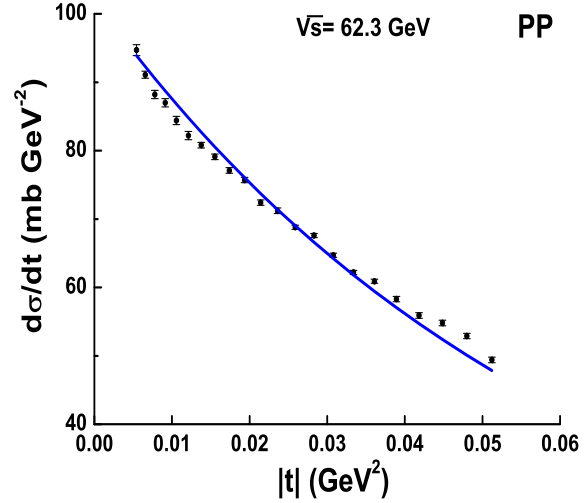


Figure 56: The points are the experimental data by N. Amos et al., Nucl. Phys. **B262** (1985) 689.

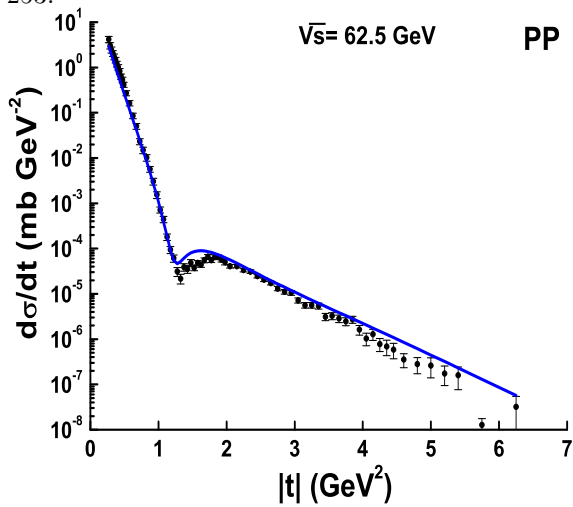


Figure 57: The points are the experimental data by U. Amaldi and K.R. Schubert, Nucl. Phys. **B166** (1980) 301.

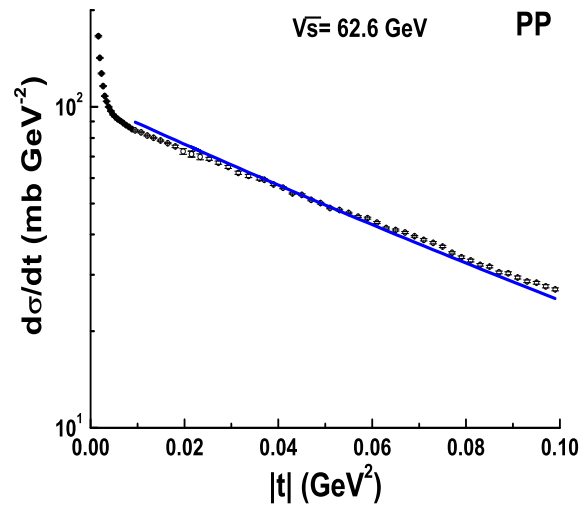


Figure 58: The points are the experimental data by U. Amaldi and K.R. Schubert, Nucl. Phys. **B166** (1980) 301.

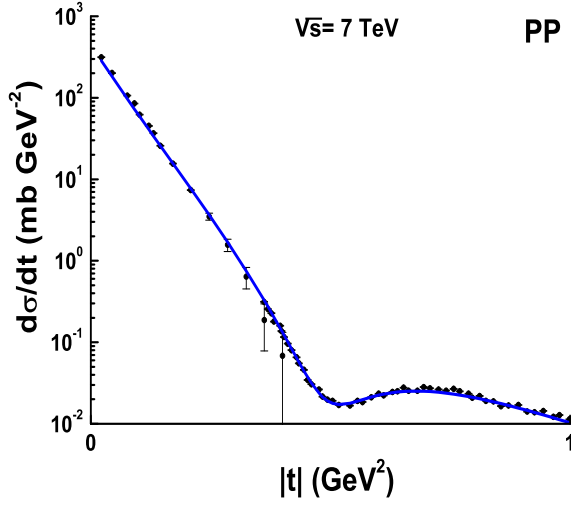


Figure 59: The points are the experimental data by the Totem Collaboration (G. Antchev et al., Europhys. Lett., **96**, 21002 (2011); Europhys. Lett., **95**, 41001 (2011)) digitized by us.

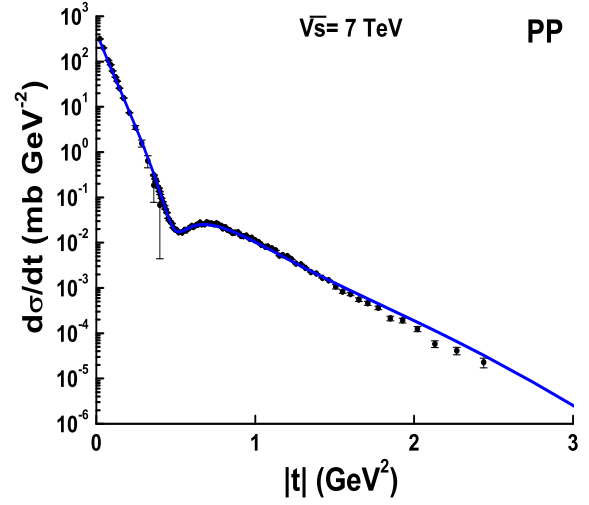


Figure 60: The points are the experimental data by the Totem Collaboration (G. Antchev et al., Europhys. Lett., **96**, 21002 (2011); Europhys. Lett., **95**, 41001 (2011)) digitized by us.

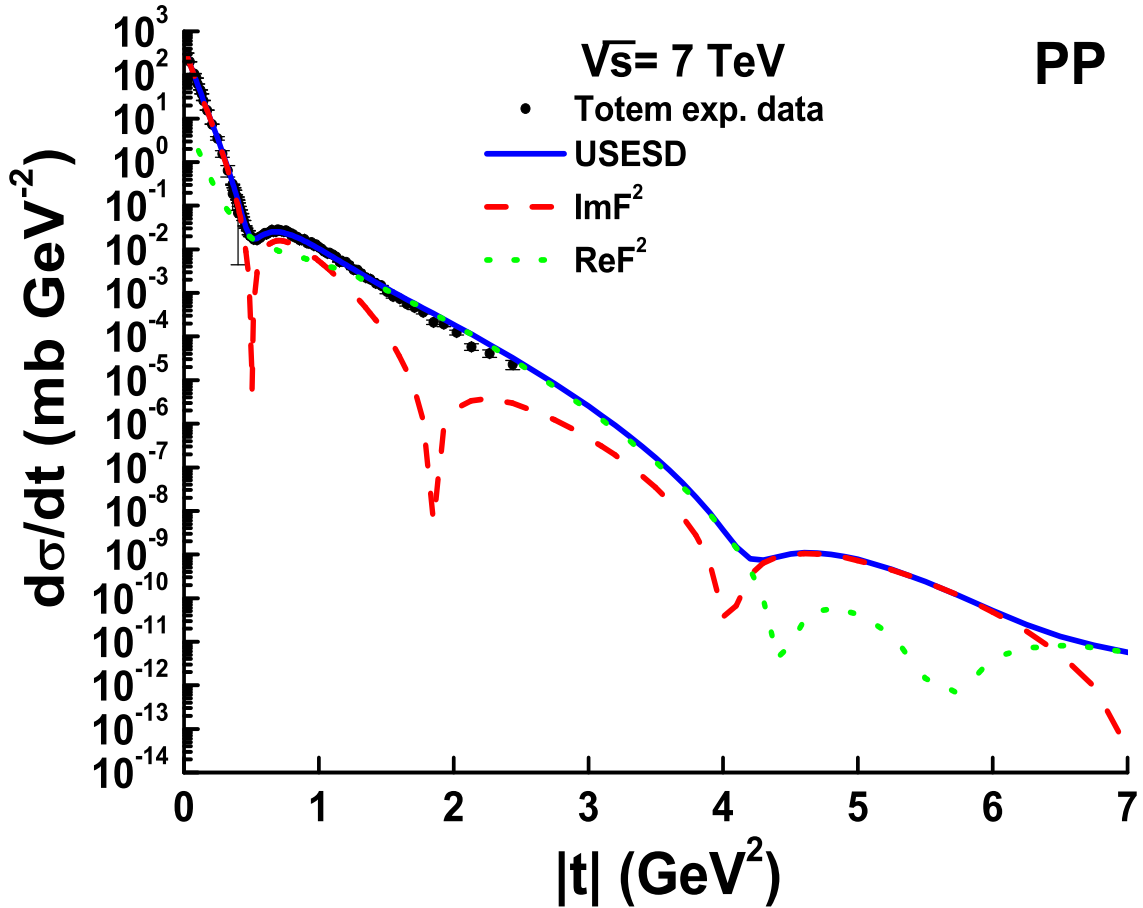


Figure 61: The points are the experimental data by the Totem Collaboration (G. Antchev et al., Europhys. Lett., **96**, 21002 (2011); Europhys. Lett., **95**, 41001 (2011)) digitized by us.